Regional Lung Water Measurements with PET: Accuracy, Reproducibility, and Linearity

Marissel Velazquez, John Haller, Thor Amundsen, and Daniel P. Schuster

Respiratory and Critical Care Division, Department of Internal Medicine, Washington University School of Medicine, St. Louis, Missouri

We evaluated the accuracy, reproducibility, and linearity of lung water concentration (LWC) measurements using positron emission tomography (PET) in anesthetized supine dogs. First, we evaluated whether errors in attenuation correction, which might occur during the development of pulmonary edema, significantly affect LWC and pulmonary blood flow (PBF) measurements obtained with PET. In 10 animals, PET scans of LWC and PBF were obtained before and after oleic acid induced lung injury. Changes in LWC and PBF after injury were underestimated by 12%–25% if the postinjury LWC scan was reconstructed using attenuation data obtained prior to injury, before lung density had changed, instead of attenuation data obtained after lung injury. Next, in four other dogs, we did not administer oleic acid, but instead instilled progressive amounts of autologous plasma into the left caudal lobe and obtained LWC measurements after each. Changes in LWC were linearly related to the amount of plasma instilled ($r = 0.99$). The average coefficient of variation for LWC in the control right lobe was $4 \pm 2\%$ and the average percent change between measurements was $1.5\% \pm 5.8\%$. The correlation of regional LWC determined gravimetrically after the last scan, when corrected for differences in regional lung density, with LWC determined by PET, was excellent ($r = 0.92$). We conclude that when the correct attenuation scan is used for emission scan reconstruction, PET measurements of LWC are accurate, linear, and reproducible.

J Nucl Med 1991; 32:719–725

In a previous study (*1*), we reported a technique for measuring regional extravascular lung water (EVLW) concentration using positron emission tomography (PET) and oxygen-15-labeled tracers of water and carbon monoxide. In two subsequent studies, we evaluated the effect of pulmonary blood flow on the EVLW measurement (*2*) and also provided validation data by comparing the technique with gravimetric measurements of EVLW (*3*). Several other important technical issues, however, have not been addressed previously.

For instance, each PET study is normally begun by obtaining an attenuation scan of the body in the field of view. This scan is used to correct subsequent emission scans for potential errors due to tissue attenuation of radioactivity. In addition, the attenuation of emitted annihilation photons is largely proportional to tissue density (*4,5*). Thus, typically, only one such scan is performed during a PET study, as for instance in cardiac or neurologic applications, even if multiple emission scans will be obtained, because no significant change in tissue density is expected between such scans.

The situation in pulmonary studies is potentially quite different. Not only does tissue density vary greatly within the thorax, but it can change dramatically as a result of EVLW accumulation, atelectasis, etc. Consequently, in all our previous studies we have measured the attenuation of radioactivity by thoracic tissues after any intervention which could result in a change in tissue density. Such maneuvers require additional time and result in additional radiation exposure. It is unclear whether ignoring changes in attenuation (e.g., such as those that occur after lung injury) will significantly affect the accuracy of lung water concentration (LWC) and pulmonary blood flow (PBF) measurements. The magnitude of error in subsequent emission scans from failing to correct for attenuation changes is not known.

In addition, although in a previous study we correlated the EVLW measurement in both normal and abnormal lung with gravimetrically determined measurements (*3*), questions concerning linearity or the minimum difference needed to detect a change in EVLW were not addressed. The latter issue is especially pertinent since we have observed an increased rate of extravascular protein accumulation after acute lung injury, consistent with increased pulmonary vascular permeability, but have not always observed increased EVLW accumulation in the same regions (*6,7*). Furthermore, the validation data were obtained from only eight animal experiments.

The purpose of the present study, then, is to address three issues: (1) to determine whether a second attenuation scan is necessary if lung density has changed between emission scans; (2) to evaluate the linearity and reproducibility of our PET technique for measuring changes in LWC (including the minimum difference required to detect a change); and (3) to broaden the data base used to validate the PET measurement of EVLW.

Received Jul. 30, 1990; revision accepted Oct. 30, 1990.

For reprints contact: Marissel Velazquez, MD, Pulmonary Division, St. Louis University Medical Center, 3635 Vista at Grand, PO Box 15250, St. Louis, MO 63110-0250.

METHODS

Animal Preparation

Studies were performed on 14 healthy adult mongrel dogs, of either sex, weighing 23–31 kg. Anesthesia was induced with i.v. pentobarbital sodium (25–30 mg/kg). All animals were also paralyzed with i.v. pancuronium bromide (4 mg). After intubation with a cuffed endotracheal tube, mechanical ventilation was initiated using a Harvard pump respirator at a tidal volume of 15 ml/kg and an FiO2 of 1.0. The respiratory rate was adjusted to keep the arterial pH and PCO_2 within the normal range. Additional anesthetic and muscle relaxant were administered when necessary.

An external jugular vein catheter was used for administering drugs and radiopharmaceuticals. Through bilateral femoral incisions, a balloon-tipped (7 Fr) and a pig-tailed (6.3 Fr) catheter were positioned in the pulmonary artery under fluoroscopic guidance. An indwelling 7-cm (18 gauge) catheter was placed in the femoral artery for blood sampling. Transducers (Gould P-50) were calibrated to the center of the lateral chest and connected to a Mennen model 742 monitor for systemic arterial pressure and pulmonary artery and wedge pressure recordings. Cardiac output was measured in triplicate by the thermodilution technique. Blood gas analysis was performed on an Instrumentation Laboratories model 813 blood gas analyzer.

In addition, in 4 of the 14 dogs (PLASMA group, see experimental protocols, below), 60 cc of blood was drawn into a heparinized syringe (10 units of sodium heparin/cc of blood) and centrifuged for 10 min (2,500 rpm) at 10°C. In these animals, a tracheostomy was also performed and a 4-mm internal diameter microlaryngeal endotracheal tube (National Catheter, without the balloon cuff) was positioned under fluoroscopy into the left caudal lobe (LCL) bronchus for instillation of autologous plasma. A rubber cap was inserted onto the external end of the microlaryngeal tube to ensure that gas used to ventilate all other lobes by the main endotracheal tube would not escape through the microlaryngeal tube.

Experimental Protocols

Acute Lung Injury Groups. These animals were used to evaluate the impact of changed attenuation data on LWC and PBF measurements. Baseline data included:

1. A blank and body attenuation scans (to correct subsequent emission scans for the effects of photon attenuation).
2. A 15-sec scan for the PBF measurement.
3. A 300-sec scan for the partition coefficient (necessary for the PBF calculation) and LWC measurements.
4. Hemodynamic and blood gas analysis data.

All measurements were obtained in about 15–20 min.

In five dogs (LOBAR group), after all baseline measurements were performed, oleic acid (0.015 ml/kg) diluted in 3 cc 70% EtOH (for a better dispersal of the small volume of oleic acid used) was administered to the LCL through the distal tip of a balloon-wedged pulmonary catheter (*6,8*). The catheter was flushed with 10 cc of saline and the balloon was deflated. Data from the uninjured contralateral (RCL) lobe were used as controls. Sixty minutes after oleic acid administration, all measurements were repeated.

In five other animals (DIFFUSE group), oleic acid (0.08 ml/kg diluted in 5 cc of saline) was administered into the right atrium through the infusion port of a pulmonary catheter. This technique results in widespread injury to all lung lobes (*6*). Data sets were obtained at baseline and 60 min after oleic acid infusion.

To evaluate the impact that errors in attenuation correction might have on PBF and LWC measurements, all postinjury PBF and LWC images were reconstructed twice: first with the baseline (preinjury) attenuation scan data, and second with the postinjury attenuation scan data.

Physiologic data from these two groups of dogs have been reported previously (*6*).

Plasma Instillation Group

These animals were used to evaluate the linearity and reproducibility of LWC measurements and their correlation with gravimetric data. Repeat PET measurements were obtained at baseline and after sequential instillation of 1, 4, 5, and 10 cc of autologous plasma into the LCL bronchus in the four animals comprising the PLASMA group (*9*). The PET measurements (including repeat attenuation scans) were performed 5 min after each instillation. Consequently, a total of 1, 5, 10, and 20 ml of plasma had accumulated in the LCL after the first, second, third, and fourth instillation, respectively. Each data set was obtained in about 15–20 min. Plasma was used because it has previously been shown by others that the rate of plasma absorption from the lung is <5% per hour over at least 4 hr (*10*). After all PET data were collected, the animals were killed (within 30 min from the last PET measurement) for gravimetric determination of lung water content.

PET Techniques

All PET measurements were performed using a PETT-VI system. Design features, methods for calibration, decay correction of activity, and correction for photon attenuation have all been discussed in detail elsewhere (1,3,5,11–13). The PETT-VI device is a circular positron tomograph consisting of four rings of 72 cesium fluoride detectors. The field-of-view is reconstructed at 27 cm. Direct and cross-plane coincidence line data are fed to a computer and subsequently used to simultaneously reconstruct seven transverse slices with an intrinsic center-to-center separation of 1.44 cm and an in-plane full width at half maximum (FWHM) resolution of 1.17 cm. The images are reconstructed by filtered backprojection with a resolution of 1.8 cm FWHM and a pixel size of 0.27 cm × 0.27 cm.

In each study, the first tomographic measurement was performed in the transmission mode. Data were continuously collected over a 500-sec period after a $^{68}Ge/^{68}Ga$ ring-source was placed in the field-of-view. The animal and plastic shell used to support the animal were left out of the scanner during the first "blank" scan. Then the animal was positioned supine in the scanner and the data collection was repeated ("attenuation" scan). Typically, 8–12 million coincidence events were recorded per slice. An image was reconstructed from profiles of the inverse log ratio of the two scans. An attenuation fraction factor was determined for each detector pair. These attenuation data were used to correct subsequent emission scans for the effects of photon attenuation by tissue. Since a linear correlation exists between the values assigned to each pixel in the attenuation image (expressed in arbitrary PETT numbers) and tissue density (*4,5*), an image of tissue density distribution (g/ml) was also obtained from this procedure.

Pulmonary Blood Flow and Lung Water Measurements

Our methods for measuring both PBF and regional lung water (LWC) after a single infusion of ^{15}O-water with PET have been

described in detail elsewhere (*1,11,12*). Briefly, we used PET to measure the concentration distribution of intravenously administered ^{15}O-water. Data were collected in two phases. A 15-sec scan was performed during a 20-sec constant infusion of ^{15}O-water ($2.2–3.0 \times 10^5$ MBq). Typically 0.3–0.5 million coincidence events were recorded per slice. This first measurement represented the initial distribution of the tracer in the pulmonary circulation and is directly related to PBF. Four minutes later, once ^{15}O-water in blood and lung tissue were at equlibrium, a 300-sec data collection followed. Here, about 1.5–2.0 million coincidence events were recorded per slice. Values obtained from this latter scan were used to determine the apparent regional partition coefficient for the tracer (necessary for the PBF calculation) and to measure LWC. During both periods of data collection, blood samples were drawn (continuously during the first 15 sec scan, and every 30 sec during the second scan) and their radioactivity measured in a well counter. PET measurements of activity were calibrated against activity measurements from this same well-counter. The blood activity data, and tissue activity measurements obtained with the PET scanner were analyzed with a one-compartment mathematical model to yield quantitative tomographic images representative of PBF. LWC was calculated by first referencing the radioactivity in any given lung region on the scan to activity in blood samples taken during the scan and then by assuming a value of 0.84 ml water/ml blood or lung tissue. Thus, $rLWC = 0.84\ C_{PET}/\int_{T_1}^{T_2} C_B\ (t)dt$ where C_{PET} = lung tissue radioactivity (counts/ml lung) integrated over the duration of the scan, and C_B = blood activity (counts/ml blood) in multiple peripheral blood samples obtained from the start (T_1) to the end (T_2) of the scan period.

In the PLASMA group of animals, intravascular water (IVW) was also measured using inhaled ^{15}O-labeled carbon monoxide as a blood-pool marker (*1,12*). IVW was calculated, again, by referencing the scan data to peripheral blood activity data and by assuming a water content of 0.84 ml/ml of blood.

Finally, EVLW was calculated by simply subtracting regional IVW from LWC.

Gravimetric Determination of Lung Water

These measurements were performed employing a modification of methods described by others (*3,14*). Briefly, 90 min before the scanning period was completed in the PLASMA group (see below), approximately 20 ml of blood was drawn from one of the available catheters for ^{51}Cr red blood cell labeling (New England Nuclear NEZ-030). Labeled cells were reinfused into the animal 5–10 min before the end of all imaging. Following intravascular equilibration of the labeled cells for 10 min, a peripheral blood sample was obtained.

At the end of the PET imaging period, appropriate ventilatory support was maintained until the animal was killed with i.v. saturated KCl. Ventilation was then stopped at end-expiration with the airway closed. A midline sternotomy was performed, the lungs were clamped at the hila and excised, one at a time, and quickly immersed in liquid nitrogen. Sufficient time was allowed for the tissue to solidify without becoming hard and brittle. As expected, this procedure resulted in tissue shrinkage in all directions.

With the help of a plastic outline, using anatomic landmarks as a reference, tissue slices were obtained that corresponded to the two contiguous slices on the PET image closest to the dome of the diaphragm (see following section). From each slice, lung tissue was excised that corresponded to regions of interest (ROIs) on the PET image. The pleural surface was excised from each tissue cube, and then 1–3 g lung from each cube was placed in appropriately labeled counting vials. Large central airways and vessels were excluded.

Each vial was weighed and then placed into a gamma scintillation counter along with weighted samples of peripheral blood. Counts per minute of ^{51}Cr were recorded for each sample of lung tissue and blood. All samples were then dried to a stable weight in an oven at 70°C over 7–10 days. Results were expressed as the ratio of extravascular water content to bloodless dried tissue (the classic "wet-to-dry" weight ratio).

Data Analysis

The three tomographic slices closest to the diaphragm were analyzed from each dog that received oleic acid (LOBAR and DIFFUSE groups), since these image slices have the greatest amount of lung tissue and the least amount of heart or mediastinal structures. Previously, postmortem studies have demonstrated these slices to be within the caudal lobes (*8*). For each slice, ROIs in the left and right dorsal halves of the baseline transmission scan (Fig. 1, upper left) were drawn along the inner boundary of the areas of highest density (i.e., along the dorsal boundary of the lung). These regions corresponded to the PBF images obtained at baseline (Fig. 1, lower left). Mean values for each region were obtained for all PET measurements performed. Data from postinjury emission images of PBF and LWC, reconstructed with data from the postinjury attenuation scan, were compared with the same postinjury images reconstructed instead with the attenuation data obtained at baseline. Values obtained from the LCL in the LOBAR group and values obtained from

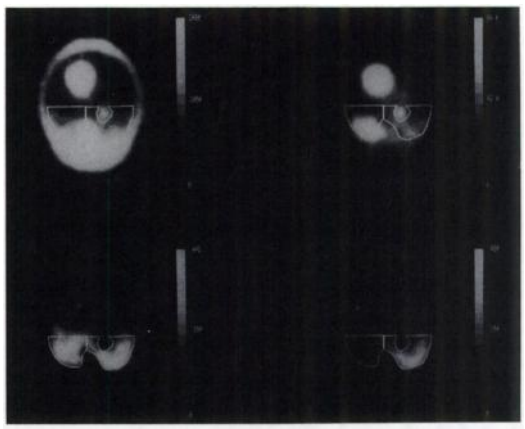

FIGURE 1. Single tomographic transverse PET images obtained from one supine dog from the LOBAR group. The image is at the mid-ventricular level (large white circular object within the lung fields). The left side of the image is the left side of the animal. The top of the image is the ventral aspect of the animal. (Upper left) An attenuation image obtained at baseline. Scale is in arbitrary PET units, proportional to tissue density. Two dorsal ROIs used for data analysis are shown. (Upper right) Equilibrium LWC image, obtained *after* injury. The scale is in units of ml H_2O/100 ml lung. Higher LWC values are clearly seen in the dorsal ROI within the LCL. (Lower left) Pulmonary blood flow image obtained *before* lung injury. Scale is in units of ml/min/100 ml lung. Blood flow is approximately equal in the two dorsal ROIs. (Lower right) Pulmonary blood flow image *after* lung injury to the left caudal lobe. A reduction of blood flow to the injured lung is clearly evident. All emission images in this figure were reconstructed with the correct attenuation data.

the DIFFUSE experiments were compared with results obtained from the control (RCL) lobe in the LOBAR group.

In the plasma instillation studies (PLASMA group), regions of lung showing an increase in water concentration were determined by subtracting the baseline LWC image from images obtained after each plasma instillation. A ROI from the one tomographic slice showing the greatest increase in LWC after 20 cc of plasma instillation was chosen for analysis (Fig. 2). Subsequently, the LWC values for this region were obtained retrospectively in each of the images obtained after each level of plasma instillation. As a control, a comparable region, at the same gravitational level, was defined on the same tomographic slice on the right side.

In addition, in the PLASMA group, EVLW values were determined for ROIs defined on the two tomographic slices closest to the dome of the diaphragm. The diaphragmatic boundary was visualized on the attenuation image by observing the difference between lung density above the diaphragm and tissue density (liver and spleen) below the diaphragm. These ROIs were large, dividing each lung into equal thirds in the ventral-dorsal direction, and in half along the medial-lateral axis. EVLW data from these ROIs were compared with EVLW data determined gravimetrically from the tissue samples described above. A total of 86 regions (20–22 regions per dog) were analyzed from both the LCL and RCL.

LWC and EVLW are expressed as ml water/100 ml lung. PBF is reported in ml/min/100 ml lung. Lung density units are in g/100 ml.

To test for statistically significant differences between mean values, the General Linear Model Procedure of the Statistical Analysis System (SAS Inc., Cary, NC) was used to perform a repeated measures analysis of variance. Post-ANOVA, t-tests were then conducted among previously chosen pairs of least-square means. Correlations were performed by standard least-squares linear regression. Reproducibility was evaluated by calculating the coefficient of variation between repeat measurements under the same conditions and by calculating an intraclass correlation coefficient. The latter is simply the correlation coefficient for all possible pairs of repeat measurements within each dog. We accepted $p < 0.05$ as indicating statistical significance. Data are presented as the mean ± 1 s.d.

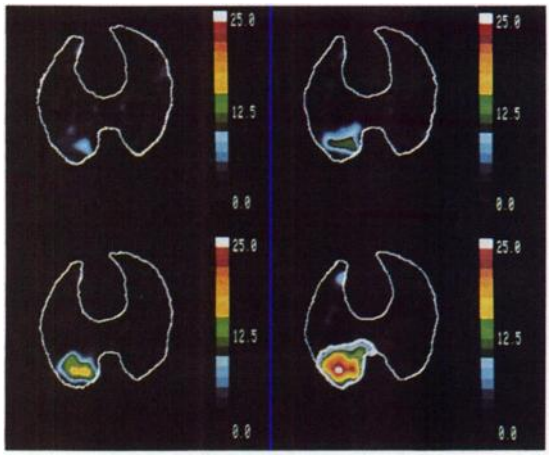

FIGURE 2. Subtraction PET images of change in LWC from one animal in the PLASMA group. The white outline represents the chest wall and cardiac fossa borders from one tomographic image at the mid-ventricular level. The area within the region therefore represents lung tissue. Image orientation is as in Figure 1. Each image represents the difference in LWC before and after instillation of autologous plasma into the LCL. (Upper left) After 1 ml plasma. (Upper right) After an additional 4 ml plasma. (Lower left) After an additional 5 ml plasma. (Lower right) After an additional 10 ml of plasma. Scales are in units of ml H_2O/100 ml lung. A progressive increase in LWC after each instillation is clearly seen. The ROI used to calculate change in LWC is shown in the lower right image.

RESULTS

Acute Lung Injury Groups

As previously reported (*6*), 1 hr after oleic acid in the DIFFUSE group, lung density increased significantly in both caudal lobes (from 54 ± 7 to 66 ± 12 and from 50 ± 6 to 65 ± 8 g/100 ml for the LCL, and RCL, respectively). In the LOBAR group, LCL density increased significantly (from 45 ± 4 to 67 ± 6 g/100 ml), whereas in the control lobe (RCL) it remained unchanged (45 ± 3 to 49 ± 3 g/100 ml).

Pulmonary blood flow and lung water measurements obtained 1 hr *after* injury from the DIFFUSE and LOBAR groups are summarized in Table 1. Using the correct postinjury attenuation scan to reconstruct the postinjury LWC and PBF images, LWC was higher in all affected lobes when compared with LWC in the control RCL from the LOBAR group. In addition, a significant reduction in PBF to the injured area (LCL) was observed in the LOBAR group (Fig. 1), as previously reported (*6*).

When, however, the same LWC and PBF images obtained after oleic acid were reconstructed using incorrect *preinjury* attenuation data, LWC and PBF were significantly underestimated (by 12%–25%) in injured areas of lung (compared with the same LWC and PBF data reconstructed using the *postinjury* attenuation scan) (Table 1). In the RCL of the LOBAR group (where lung density did not change), LWC and PBF did not change significantly, despite the use of the incorrect attenuation data.

TABLE 1
Lung Water and Pulmonary Blood Flow Data After Oleic Acid Injury

	DIFFUSE		LOBAR	
	LCL	RCL	LCL	RCL
LWC-AI	51 (10)‡	51 (5)‡	52 (7)‡	37 (3)
LWC-AB	43 (5)*‡	44 (3)*‡	39 (5)*	37 (2)
PBF-AI	252 (80)	190 (45)	85 (44)†	275 (63)
PBF-AB	219 (62)*	164 (43)*	64 (37)†	265 (63)

LWC-AI and LWC-AB = postinjury lung water values from images reconstructed using after injury (AI) and after baseline (AB) attenuation data, respectively (in ml/100 ml lung). PBF-AI and PBF-AB = postinjury pulmonary blood flow values from images also reconstructed with AI and AB attenuation data respectively (in ml/min/100 ml lung).

* $p < 0.05$ compared with AI image.

† $p < 0.05$ compared with RCL.

‡ $p < 0.05$ compared with LWC-AI from RCL.

Data are presented as mean (1 s.d.).

Plasma Instillation Group

To evaluate linearity and reproducibility, we analyzed the tomographic slice in this group which eventually showed the greatest change in LWC. We then drew a ROI around this area of change, as shown in Figure 2. Next, we determined the change in LWC within this ROI on each LWC scan obtained after 1, 5, 10, and 20 ml of instilled plasma had accumulated into the LCL. The results are shown in Figures 3 and 4.

In all four dogs, a linear increase in LWC was seen over the range of instilled plasma (Fig. 3). The average correlation coefficient, "r," was 0.99. Figure 4 shows the percent change in LWC over the range of instilled plasma, in both the ROI from the LCL and a region of comparable size from the RCL (control lobe). One milliliter of instilled plasma into the LCL did not result in a significant change in LWC compared with baseline values, or when compared with values from the RCL. However, 5 ml of instilled plasma resulted in an easily detectable change in LWC.

In the RCL, changes in LWC were not significantly different from baseline (Fig. 4). The average percent change between all five sequential measurements was 1.5% ± 5.8%. The average coefficient of variation among the dogs for these LWC measurements was 4% ± 2%, and the intraclass correlation coefficient was 0.96 ($p < 0.001$).

After instillation of a total of 20 ml of plasma, the animal was killed and tissue obtained for gravimetric analysis. The gravimetric data are presented in Figure 5. In this figure, data from the medial and lateral regions have been averaged at each gravitational level. In the RCL, measurements made at all three tissue levels (dorsal, middle, ventral) were comparable and similar to previously reported normal tissue values (*3,14*). In the LCL, the wet-to-dry weight ratio was higher in the dorsal and middle regions, in the area of the instilled plasma, than in the ventral region.

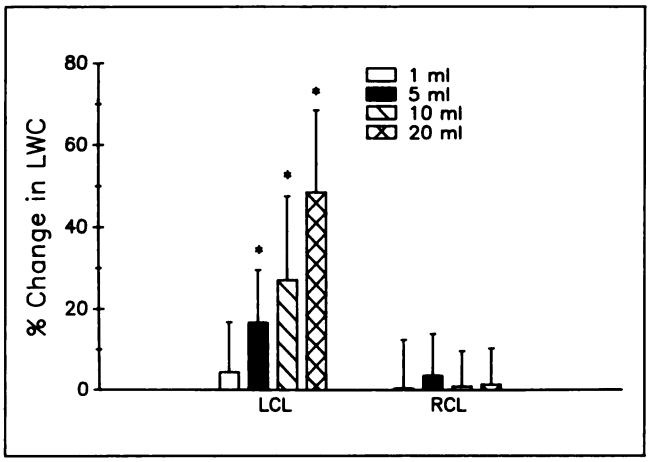

FIGURE 4. The mean (± 1 s.d.) percent change from the baseline lung water concentration after each instillation of autologous plasma for all four dogs in the PLASMA group, based on data shown in Figure 3 and including comparable data for the right caudal lobe. * = $p < 0.05$ compared with baseline, with changes in the left lung after 1 cc of plasma, and with the mean changes in similar ROIs in the right lung obtained at the same time.

EVLW data obtained with PET from comparable regions on the PET images are also shown in Figure 5. Here, unlike the gravimetric data in the RCL, EVLW is higher in the dorsal region. This is to be expected as the PET data are expressed in terms of *lung volume*, and lung tends to be compressed and/or atelectatic in dorsal regions in supine dogs. In the LCL, like the gravimetric data, EVLW is higher in the dorsal region than in the ventral region or the comparable region in the RCL. Also like the gravimet-

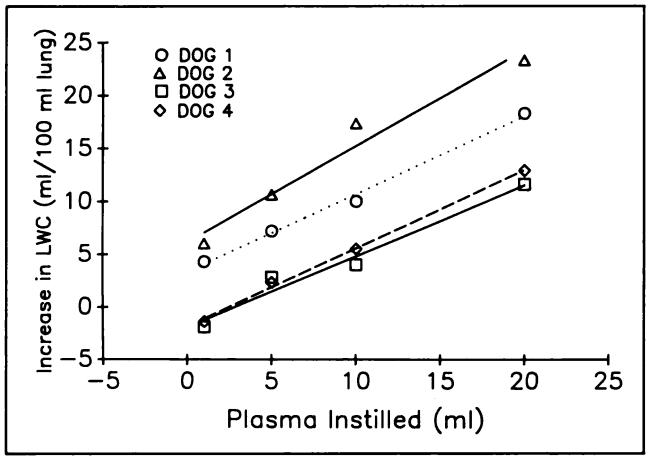

FIGURE 3. Changes in LWC after each instillation of autologous plasma in each dog of the PLASMA group. The ROIs used to determine the change in LWC are similar to that shown in Figure 2. There is a linear and proportionate increase in LWC after each instillation in each dog. The lines shown are the regression lines for each set of individual dog data.

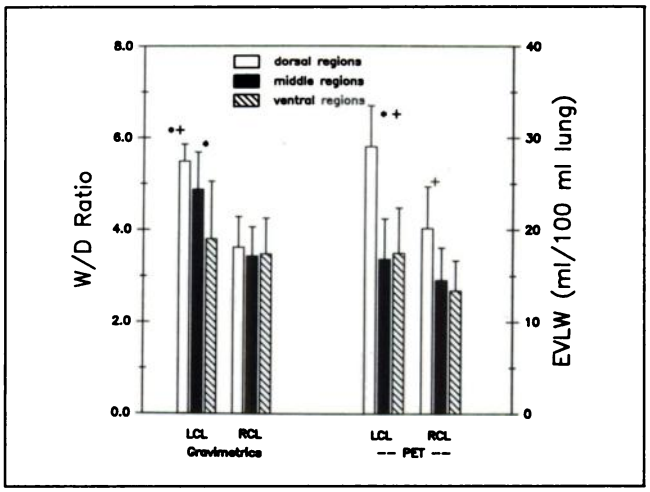

FIGURE 5. Gravimetric lung water data (expressed as the extravascular wet-to-bloodless dry lung weight, i.e., W/D, ratio) and PET EVLW measurements obtained from ROIs on the PET images corresponding to the tissue samples used for the gravimetric data. * = $p < 0.05$ compared with the comparable region in the contralateral lung. + = $p < 0.05$ compared with the ventral region in the ipsilateral lung.

ric data, there is no significant difference between ventral regions. Thus, the major difference in the pattern of PET and gravimetric data occurred in the middle region.

In an attempt to account for the differences in pattern between the gravimetric and PET data, the water content of the tissue sample (ml H_2O/gm lung) was multiplied by its density (gm lung/ml lung), obtained from the tomographic attenuation scan (*3,4*). The correlation of total regional LWC determined by PET with the similar measurement made gravimetrically is shown in Figure 6. The correlation is excellent with a correlation coefficient of r = 0.92. The regression equation relating these two methods is LWC − Gravimetrics = 0.96 (LWC − Gravimetrics PET) + 0.06 for all 86 tissue samples obtained in all four dogs. The gravimetric and PET data are both expressed as ml H_2O/ml lung. However, the correlation between the two PET measurements themselves (LWC and density) was equally strong: r = 0.90.

The correlation of the PET measurement of *extravascular* water (EVLW) with similar measurements determined gravimetrically is also shown in Figure 6. Here the correlation was r = 0.86. The regression equation relating the two methods is EVLW − Gravimetrics = 1.15 (EVLW − PET) + 0.03.

DISCUSSION

Our data clearly show that an attenuation scan is necessary before each emission scan when pulmonary parenchymal tissue density has changed between scans. For instance, after oleic acid induced pulmonary edema, the LWC increased about 37%, on average, in the affected lung regions. However, if the lung water scan was reconstructed with the *baseline* attenuation scan data (as is the case in non-pulmonary PET studies), serious underestimation of the postinjury lung water images was recorded

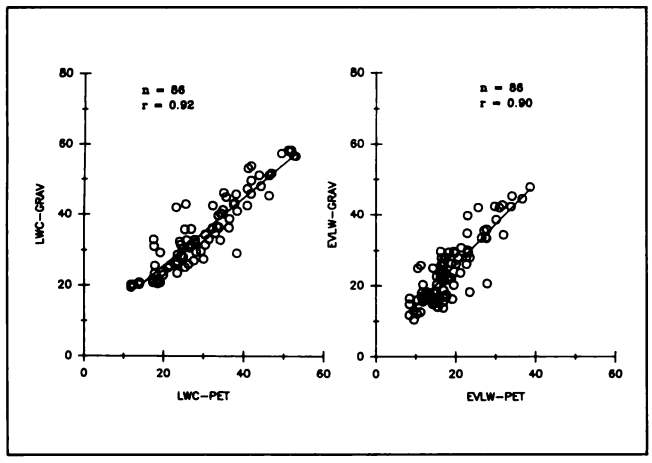

FIGURE 6. (Left) The correlation of total regional LWC measurements obtained with PET (LWC-PET) with similar measurements obtained gravimetrically (LWC-GRAV). See text for equation of the regression line. (Right) The correlation of regional EVLW measurements obtained with PET in the same regions as the left half of the figure with similar measurements obtained gravimetrically. See text for equation of the regression line.

(Table 1). Indeed, in the LOBAR group, this "incorrect" value for LWC in the injured left lung was indistinguishable from the truly unaffected right caudal lobe (Table 1). Errors encountered for the pulmonary blood flow measurements were comparable. Thus, it is possible for pathologic changes to be missed completely, if attenuation data change during the course of a study, but are unappreciated, and the incorrect attenuation data are then used in reconstructing the subsequent emission scans. As in this study with experimental edema, lung attenuation as measured by PET also increases significantly during human pulmonary edema (*15*).

The attenuation scan is used to calculate an attenuation fraction factor for each detector pair. This factor represents the fraction of photons from an external positron source which are attenuated by tissue, and is used to "scale-up" the regional tissue activity data in any subsequent emission scan along the line of projection between the two coincident detectors. If true tissue density is greater than that recorded from the baseline attenuation scan, as it would be after lung injury leading to pulmonary edema, then the regional tissue activity data in the emission scans will be underestimated. This is indeed the kind of error found in our study. Although repetitive transmission scans add to the time and complexity of any PET study, it is now clear that they must be performed to obtain accurate data.

Several previous studies have evaluated the use of PET to measure lung density (*4,5*). In both cases, the correlation of PET measurements of lung density with the known density of various large phantoms is extremely good (r = 0.99) (*5*). However, the measurement of lung density in vivo is more problematic because of scattered radiation effects and partial-volume averaging errors. The latter are especially important because of the wide variation in tissue densities within the thorax and the poorer spatial resolution of PET. Indeed, Schuster et al. (*5*) estimated that perhaps 50% of the differences between PET and x-ray CT measurements of lung density were due to overestimates of lung density from partial-volume averaging errors.

Data from the RCL in the PLASMA group allow us to address the issue of reproducibility. The average coefficient of variation among the different animals for repeat measurements from the RCL was 4% ± 2% [which obviously compares favorably with the 3% value reported in a previous study (1)], and the intraclass correlation co-efficient was also highly significant (r = 0.96). These data, with data from Figure 4, also allow us to evaluate the minimum change in LWC detectable by PET. Since the average percent change between LWC measurements in the unaffected RCL was 1.5% ± 5.8%, changes greater than 6%–12% (1–2 s.d.) should be reliably detected compared with background levels of noise. This indeed seems to be the case, as the average percent change in LWC after only 5 ml of instilled plasma was 17% ± 13% and was significantly different from both baseline values and values obtained at the same time in the RCL. These data are

reassuring, since in previous studies we failed to find increases in lung water in some lung regions after oleic acid injury, even though measurements of transvascular protein flux suggested the presence of significant increased vascular permeability (*6,7*). Thus, it is likely, given the data in the current study, that the failure to detect an increase in LWC in those previous studies indicates that modest increases in transvascular protein flux can occur before significant edema accumulates, and not because of poor LWC measurement sensitivity per se.

Finally, the gravimetric PET lung water correlations expand our data base for validating the accuracy of the lung water measurement (*3*). Despite the high correlation, direct comparison (without a density correction) in Figure 5 shows that some differences exist. Some of this difference may reflect misregistration between tissue samples from the gravimetric analysis and ROIs on the PET images. Since the ROIs were large, we doubt this error was important in either the ventral-dorsal or medial-lateral direction. Misregistration between *adjacent* regions (for instance, between the middle and either dorsal or ventral regions or between tomographic slices) is more likely. This may explain some of the differences seen in Figure 5 (see below). Obtaining the PET images in a non-respiratory gated mode may have also contributed to this kind of error, but only if the *physiology* between adjacent slices differed significantly. Such errors were minimized by knowing that the plasma was injected directly into the left caudal lobe, and choosing slices in reference to a specific landmark (the diaphragmatic surface).

To adjust the gravimetric data for the effect of regional differences in tissue inflation, we multiplied the gravimetric water content of each sample by the tissue density determined with PET. The impact of this "correction" is seen in comparing Figure 5 with Figure 6. In Figure 5, for both gravimetrics and the PET EVLW data, values from the dorsal region in the LCL were significantly different from comparable regions in the contralateral lung or the ventral regions in the ipsilateral lung. Likewise, for both measurement techniques, there was no difference between ventral regions between the two lungs. Also, there was no difference between middle and ventral regions on the left side (although gravimetrically, the difference was almost significant: $p = 0.07$). The effect of inflation per se is seen most clearly by inspecting the data from the RCL alone, where there was no difference among the regions by gravimetrics (as expected) but the EVLW *concentration* of the dorsal region was greater than that of the ventral region, indicating atelectasis in the dorsal region. Interpretation of data from the middle regions is more difficult, since it probably represents the effects of both plasma instillation and regional inflation. On the other hand, interpreting the correlations shown in Figure 6 is influenced by the strong correlation between the two PET measurements themselves (LWC and density). This strong correlation exists because approximately 80% of tissue is water and both PET measurements are affected equally by differences in regional inflation.

In summary, the data from this study demonstrate the necessity of performing an attenuation scan to correct regional tissue activity measurements in subsequent emission scans whenever lung density may have changed. When the correct attenuation scan data are used, however, lung water measurements with our PET technique are linear, reproducible, and generally conform to the pattern of measurements obtained gravimetrically. Changes in lung water concentration greater than 6%–12% from the previous measurement should be reliably detected. Taken together, we believe these data suggest that PET is currently the best in vivo method for measuring regional lung water concentration (*12,16*).

ACKNOWLEDGMENTS

The authors wish to thank Lisa Schomaker for her secretarial assistance. This work was supported by NIH grant HL 32815.

Dr. Schuster is an established investigator on the American Heart Association and a career investigator for the American Lung Association. This work was performed during Dr. Velazquez's tenure as a clinical investigator of the NIH.

REFERENCES

1. Schuster DP, Mintun MA, Green MA, Ter-Pogossian MM. Regional lung water and hematocrit determined by positron emission tomography. *J Appl Physiol* 1985;59:860–868.
2. Velazquez M, Schuster DP. Effect of regional pulmonary blood flow on extravascular lung water measurements using positron emission tomography. *J Appl Physiol* 1988;65:1267–1273.
3. Schuster DP, Marklin GF, Mintun MA. Regional changes in extravascular lung water detected by positron emission tomography. *J Appl Physiol* 1986;60:1170–1178.
4. Rhodes CG, Wollmer P, Fazio F, Jones T. Quantitative measurement of regional extravascular lung density using positron emission tomography. *J Comp Assist Tomogr* 1981;5:783–791.
5. Schuster DP, Marklin GF, Mintun MA, Ter-Pogossian MM. PET measurement of regional lung density. 1. *J Comput Assist Tomogr* 1986;10:723–729.
6. Schuster DP, Haller JW, Velazquez M. A positron emission tomographic comparison of diffuse and lobar forms of acute oleic acid lung injury. *J Appl Physiol* 1988;64:2357–2365.
7. Velazquez M, Schuster DP. Relationship of extravascular lung water to measured changes in permeability: a positron emission tomography study. *Chest* 1988;93:187S.
8. Velazquez M, Schuster DP. Pulmonary blood flow distribution after lobar oleic acid injury: a PET study. *J Appl Physiol* 1988;65:2228–2235.
9. Muir AL, Hogg JC, Naimiark A, Hall DL, Chernacki W. Effect of alveolar liquid on distribution of blood flow in dog lungs. *J Appl Physiol* 1974;39:885–890.
10. Matthay MA. Resolution of pulmonary edema. *Clin Chest Med* 1985;6:521–545.
11. Mintun MA, Ter-Pogossian MM, Green MA, Lich LL, Schuster DP. Quantitative measurement of regional pulmonary blood flow with positron emission tomography. *J Appl Physiol* 1986;60:317–326.
12. Schuster DP. Positron emission tomography: theory, and its application to the study of lung disease (state-of-the-art). *Am Rev Respir Dis* 1989;139:818–840.
13. Yamamoto M, Ficke DC, Ter-Pogossian MM. Performance study of PETT-VI. A positron computed tomograph with 288 cesium fluoride detectors. *IEEE Trans Nucl Sci* 1982;29:529–533.
14. Pearce ML, Yamashita J, Beazell J. Measurement of pulmonary edema. *Circ Res* 1965;26:482–488.
15. Wollmer P, Rhodes CG, Deanfield J, et al. Regional extravascular density of the lung in patients with acute pulmonary edema. *J Appl Physiol* 1987;63:1890–1895.
16. Staub NC. Clinical use of lung water measurements: report of a workshop. *Chest* 1987;90:588–594.